Middle-East Journal of Scientific Research 10 (3): 316-321, 2011
ISSN 1990-9233

Application of a Probabilistic Neural Network in Radial Velocity Curve Analysis of the Spectroscopic Binary Stars HD 194495, BD+60497, HD 17505Aa, HDE 284414 and LZ Cep (HD 209481)

[1]*Kamal Ghaderi,* [2]*Elahe Ghasemisalehabadi,* [3]*Majid Khajvand Kiakalaee,*
[1]*Karvan Karimizadeh,* [1]*Hedayat Fatahi and* [1]*Touba Rostami*

[1]Department of Science and Engineering, Islamic Azad University, Marivan Branch, Marivan, Iran
[2]Department of Civil Engineering, Islamic Azad University, Anar Branch, Anar, Iran
[3]Department of Civil Engineering, Islamic Azad University, Chalous Branch, Chalous, Iran

Abstract: Using measured radial velocity data of five double-lined spectroscopic binary systems HD 194495, BD+60497, HD 17505Aa, HDE 284414 and LZ Cep (HD 209481) we find corresponding orbital and spectroscopic elements via a Probabilistic Neural Network (PNN). Our numerical results are in good agreement with those obtained by others using more traditional methods.

Key words: Stars · Binaries · Eclipsing · Stars · Binaries · Spectroscopic

INTRODUCTION

Analysis of both light and radial velocity (hereafter V_R) curves of binary systems helps us to determine the masses and radii of individual stars. One historically well-known method to analyze the V_R curve is that of Lehmann-Filhés [1]. Other methods were also introduced by Sterne [2] and Petrie [3]. The different methods of the V_R curve analysis have been reviewed in ample detail by Karami and Teimoorinia [4]. Karami and Teimoorinia [4] also proposed a new non-linear least squares velocity curve analysis technique for spectroscopic binary stars. They showed the validity of their new method to a wide range of different types of binary See Karami and Mohebi [5-7] and Karami *et al*. [8].

Artificial Neural Network (ANN) have become a popular tool in almost every field of science [9-13]. Probabilistic Neural Network (PNN) is a new tool to derive the orbital parameters of the spectroscopic binary stars. In this method the time consumed is considerably less than the method of Lehmann-Filhés and even less than the non-linear regression method proposed by Karami and Teimoorinia [4].

In the present paper we use a Probabilistic Neural Network (PNN) to find the optimum match to the four parameters of the V_R curves of the five double-lined spectroscopic binary systems: HD 194495, BD+60497, HD 17505Aa, HDE 284414 and LZ Cep (HD 209481). Our aim is to show the validity of our new method to a wide range of different types of binary.

The star HD 194495 is a massive spectroscopic binary and consists of an evolved, more massive and more luminous primary component and a main sequence secondary star. The primary of HD 194495 is most consistent with a B3 IV-V star while the secondary matches most closely with a B4 V star and the orbital period is P=4.90494 days [14]. The spectra of BD+60497 show clear evidence that this star is a double-lined spectroscopic binary that belongs to the cluster IC 1805. The spectral type is O6 V and O8 V for the primary and the secondary star, respectively and the orbital period is P =3.95863 days [15]. HD 17505Aa is a close binary in the multiple-star system HD 17505 that belongs to the cluster IC 1805. The spectral type is O7.5 V with a period of P=8.5710 days [15]. HDE 284414 is a double-lined system with a K2 V star and a fainter companion, with an indirectly estimated M0 spectral type, orbiting each other is a highly elliptical orbit with a period of P=589.75 days [16]. LZ Cep(HD 209481) is a double-lined spectroscopic binary and LZ Cep is a member of the Cep OB2 association and the components are of very similar spectral type: O9 V and the orbital period is P=3.070507 days [17].

Corresponding Author: K. Ghaderi, Department of Science and Engineering,
Islamic Azad University, Marivan Branch, Marivan, Iran.

This paper is organized as follows. In Sect. 2, we introduce a Probabilistic Neural Network (PNN) to estimate the four parameters of the V_R curve. In Sect. 3, the numerical results are reported, while the conclusions are given in Sect. 4.

V_r Curve Parameters Estimation by the Probabilistic Neural Network (PNN): Following Smart [18], the V_R of a star in a binary system is defined as follows

$$V_R = \gamma + K[\cos(\theta + \omega) + e\cos\omega] \quad (1)$$

where γ is the V_R of the center of mass of system with respect to the sun. Also K is the amplitude of the V_R of the star with respect to the center of mass of the binary. Furthermore θ,ω and e are the angular polar coordinate (true anomaly), the longitude of periastron and the eccentricity, respectively.

Here we apply the PNN method to estimate the four orbital parameters, γ, K, e and ω of the V_R curve in Eq. (1). In this work, for the identification of the observational V_R curves, the input vector is the fitted V_R curve of a star. The PNN is first trained to classify V_R curves corresponding to all the possible combinations of γ, K, e and ω. For this one can synthetically generate V_R curves given by Eq. (1) for each combination of the parameters:

- $-100 \leq \gamma \leq 100$ in steps of 1;
- $1 \leq K \leq 300$ in steps of 1;
- $0 \leq e \leq 1$ in steps of 0.001;
- $0 \leq \omega \leq 360°$ in steps of 5;

This gives a very big set of k pattern groups, where k denotes the number of different V_R classes, one class for each combination of γ, K, e and ω. Since this very big number of different V_R classes leads to some computational limitations, hence one can first start with the big step sizes. Note that from Petrie [3], one can guess γ, K and e from a V_R curve. This enable one to limit the range of parameters around their initial guesses. When the preliminary orbit was derived after several stages, then one can use the above small step sizes to obtain the final orbit. The PNN has four layers including input, pattern, summation and output layers, respectively (Fig. 5 in Bazarghan *et al*. [19]). When an input vector is presented, the pattern layer computes distances from the input vector to the training input vectors and produces a vector whose elements indicate how close the input is to a training input. The summation layer sums these contributions for each class of inputs to produce as its net output a vector of probabilities. Finally, a competitive transfer function on the output layer picks the maximum of these probabilities and produces a 1 for that class and a 0 for the other classes [20,21]. Thus, the PNN classifies the input vector into a specific k class labeled by the four parameters γ,K,e and ω because that class has the maximum probability of being correct.

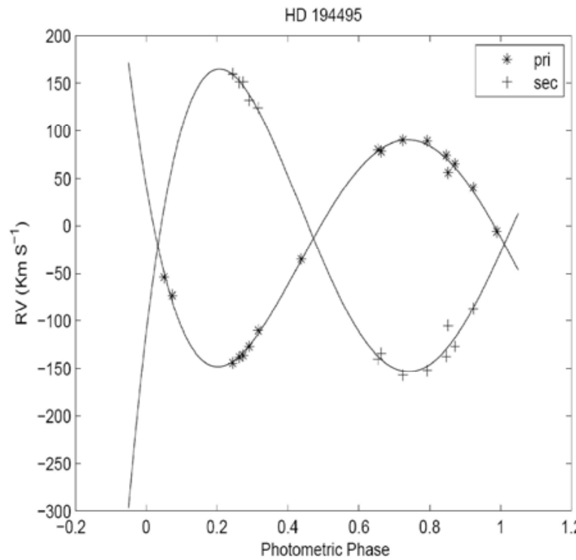

Fig. 1: Radial velocities of the primary and secondary components of HD 194495 plotted against the photometric phase. The observational data have been measured by Çakırlı *et al*. [14]

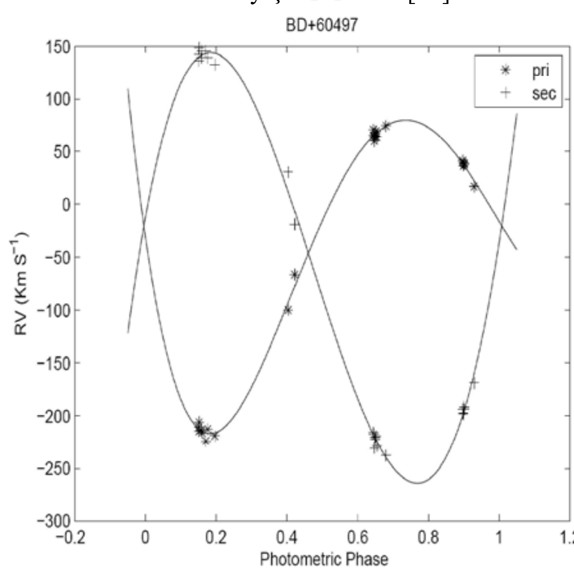

Fig. 2: Radial velocities of the primary and secondary components of BD+60497 plotted against the photometric phase. The observational data have been measured by Hillwig *et al*. [15]

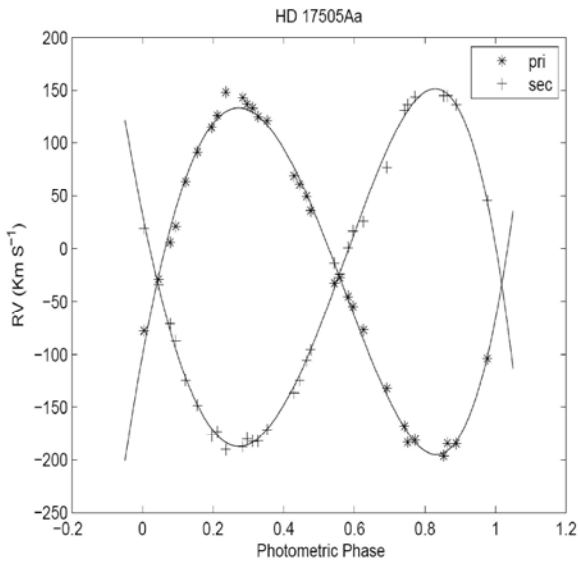

Fig. 3: Radial velocities of the primary and secondary components of HD 17505Aa plotted against the photometric phase. The observational data have been measured by Hillwig *et al*. [15]

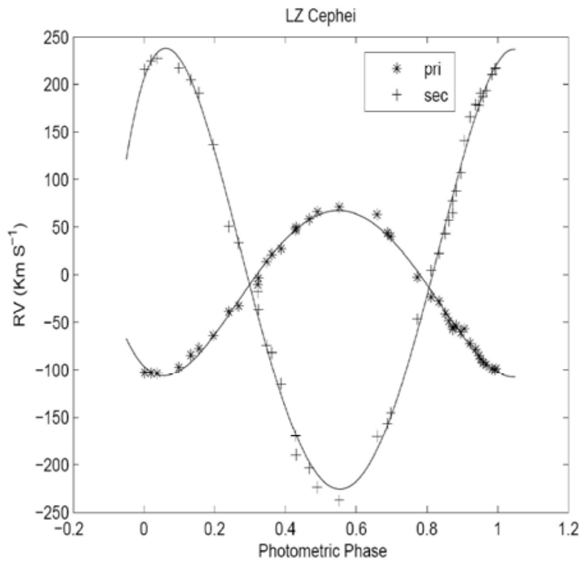

Fig. 5: Radial velocities of the primary and secondary components of LZ Cep(HD 209481) plotted against the photometric phase. The observational data have been measured by Howarth *et al*. [17]

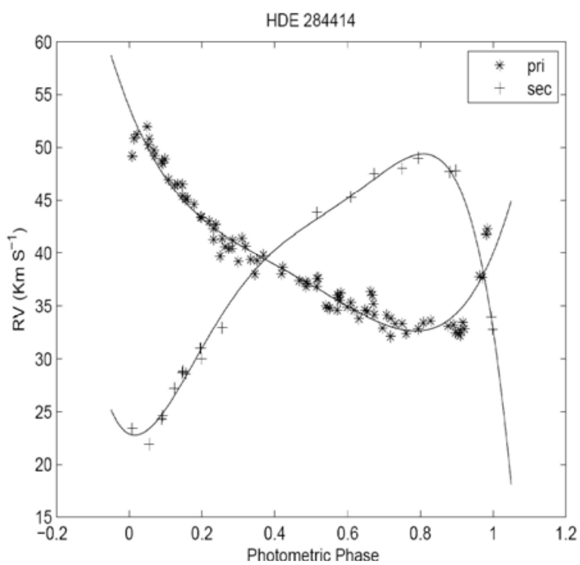

Fig. 4: Radial velocities of the primary and secondary components of HDE 284414 plotted against the photometric phase. The observational data have been measured by Tomkin [161]

Numerical Results: Here, we use the PNN to derive the orbital elements for the five different double-lined spectroscopic systems HD 194495, BD+60497, HD 17505Aa, HDE 284414 and LZ Cep(HD 209481). Using measured V_R data of the two components of these systems obtained by Çakırlı *et al*. [14] for HD 194495, Hillwig *et al*. [15] for BD+60497 and HD 17505Aa, Tomkin [16] for HDE 284414 and Howarth *et al*. [17] for LZ Cep (HD 209481), the fitted velocity curves are plotted in terms of the photometric phase in Figs. 1 to 5.

The orbital parameters obtaining from the PNN for HD 194495, BD+60497, HD 17505Aa, HDE 284414 and LZ Cep(HD 209481) are tabulated in Tables 1, 3, 5, 7 and 9, respectively. Tables show that the results are in good accordance with the those obtained by Çakırlı *et al*. [14] for HD 194495, Hillwig *et al*. [15] for BD+60497 and HD 17505Aa, Tomkin [16] for HDE 284414 and Howarth *et al*. [17] for LZ Cep(HD 209481).

Note that the Gaussian errors of the orbital parameters in Tables 1, 3, 5, 7 and 9 are the same selected steps for generating V_R curves, i.e. $\Delta\gamma = 1, \Delta K, 1\Delta e = 0.001$ and $\Delta\omega = 5$. These are close to the observational errors reported in the literature. Regarding the estimated errors, following Specht [21], the error of the decision boundaries depends on the accuracy with which the underlying Probability Density Functions (PDFs) are estimated. Parzen [22] proved that the expected error gets smaller as the estimate is based on a large data set. This definition of consistency is particularly important since it means that the true distribution will be approached in a smooth manner. Specht [21] showed that a very large value of the smoothing parameter would

Table 1: Orbital parameters of HD 194495

	This Paper	Çakırlı *et al*., [14]
γ(km/s)	-15-± 1	-15± 1
K_p(km/s)	117-± 1	116-± 4
K_s(km/s)	162± 1	161± 6
e	0.121-± 0.001	0.12-± 0.07
ω(°)	5-± 5	2.72-± 0.09

Table 2: Combined spectroscopic elements of HD 194495

Parameter	This Paper	Çakırlı *et al*. [14]
$m_p \sin^3 i/M_\odot$	6.2680-± 0.0011	6.16± 0.05
$m_s \sin^3 i/M_\odot$	4.5269-± 0.0010	4.44± 0.06
$(m_p + m_s) \sin^3 i/M_\odot$	28.0558-± 0.0021	-
$a_p \sin i/R_\odot$	11.2501-± 0.0948	-
$a_s \sin i/R_\odot$	15.5770-± 0.0942	-
$(a_p + a_s) \sin i/R_\odot$	26.8271-± 0.1890	26.68-± 0.01
m_s/m_p	0.7222-± 0.0033	0. 72

Table 3: Orbital parameters of BD+60497

	This Paper	Hillwig *et al*. [15]
γ_p (km/s)	-59-± 1	-53.8(17)
γ_s (km/s)	-59-± 1	-67.5(23)
K_p (km/s)	160-± 1	159.9(22)
K_s (km/s)	208± 1	207.7(29)
e	0.157-± 0.001	0.156(19)
ω(°)	195-± 5	100(11)

Table 4: Combined spectroscopic elements of BD+60497

Parameter	This Paper	Hillwig *et al*. [15]
$m_p \sin^3 i/M_\odot$	11.1282± 0.0014	11.1(5)
$m_s \sin^3 i/M_\odot$	8.5602± 0.0013	8.6(4)
$(m_p + m_s) \sin^3 i/M_\odot$	19.6884-± 0.0027	-
$a_p \sin i/R_\odot$	12.3533-± 0.0752	-
$a_s \sin i/R_\odot$	16.0593-± 0.0746	-
$(a_p + a_s) \sin i/R_\odot$	28.4127-± 0.1498	28.39(28)
m_s/m_p	0.7692-± 0.0019	0.770(15)

Table 5: Orbital parameters of HD 17505Aa

	This Paper	Hillwig *et al*. [15]
γ_p (km/s)	-26-± 1	-25.8(12)
γ_s (km/s)	-26-± 1	-26.3(12)
K_p (km/s)	167-± 1	166.5(18)
K_s (km/s)	171± 1	170.8(18)
e	0 094-± 0.001	0.095(11)
ω(°)	255-± 5	252(6)

Table 6: Combined spectroscopic elements of HD 17505Aa

Parameter	This Paper	Hillwig *et al*. [15]
$m_p \sin^3 i/M_\odot$	16.7102-± 0.0020	17.1(6)
$m_s \sin^3 i/M_\odot$	16.3194-± 0.0020	16.6(6)
$(m_p + m_s) \sin^3 i/M_\odot$	33.0296-± 0.0040	-
$a_p \sin i/R_\odot$	27.9169-± 0.2552	-
$a_s \sin i/R_\odot$	28.5856-± 0.2654	-
$(a_p + a_s) \sin i/R_\odot$	56.5025-± 0.5206	56.8(4)
m_s/m_p	0. 9766-± 0.0001	0. 975(15)

Table 7: Orbital parameters of HDE 284414

	This Paper	Tomkin [16]
γ(km/s)	38-± 1	38.75-± 0.02
K_p (km/s)	10-±1	9.73-± 0.03
K_s (km/s)	15-± 1	14.24-± 0.16
e	0.620-± 0.001	0.621± 0.002
ω(°)	305-± 5	302.4-± 0.

Table 8: Combined spectroscopic elements of HDE 284414

Parameter	This Paper	Tomkin [16]
$m_p \sin^3 i/M_\odot$	0.2767-±0.0001	0.241-± 0.005
$m_s \sin^3 i/M_\odot$	0.1844-± 0.0001	0.165-± 0.002
$(m_p + m_s) \sin^3 i/M_\odot$	0.4611-± 0.0002	-
$a_p \sin i/R_\odot$	63.6611-± 6.3020	61.9± 0.2
$a_s \sin i/R_\odot$	95.4917-± 6.2699	90.5± 1.0
$(a_p + a_s) \sin i/R_\odot$	159.1528-± 12.5719	-
m_s/m_p	1.5000-± 0.0222	1.46-± 0.02

Table 9: Orbital parameters of LZ Cep(HD 209481)

	This Paper	Howarth *et al*. [17]
γ(km/s)	-11± 1	-11.33± 0.78
K_p(km/s)	90± 1	89.0± 1.3
K_s(km/s)	233± 1	232.9± 1.7
e	0.030± 0.001	0. 0310± 0.0068
ω(°)	165± 5	161± 11

Table 10: Combined spectroscopic elements of LZ Cep (HD 209481)

Parameter	This Paper	Howarth *et al*. [17]
$m_p \sin^3 i/M_\odot$	7.4489-± 0.0005	7.68-± 0.12
$m_s \sin^3 i/M_\odot$	2.8773-± 0.0006	2.933-± 0.058
$(m_p + m_s) \sin^3 i/M_\odot$	10.3262-± 0.0011	-
$a_p \sin i/R_\odot$	5.3898-± 0.0339	5.396-± 0.081
$a_s \sin i/R_\odot$	13.9536± 0.0075	14.12± 0.10
$(a_p + a_s) \sin i/R_\odot$	19.3434-± 0.0414	-
m_p/m_s	2.5889-± 0.0026	2.617±0.043

cause the estimated errors to be Gaussian regardless of the true underlying distribution and the misclassification rate is stable and does not change dramatically with small changes in the smoothing parameter.

The combined spectroscopic elements including $m_p \sin^3 i$, $m_s \sin^3 i$, $(m_p + m_s) \sin^3 I$, $(a_p + a_s) \sin i$ and $\frac{m_s}{m_p}$ are calculated by substituting the estimated parameters K,e and ω in to Eqs. (3), (15) and (16) in Karami and Teimoorinia [4]. The results obtained for the five systems are tabulated in Tables 2, 4, 6, 8 and 10 show that our results are in good agreement with the those obtained by Çakırlı *et al*. [14] for HD 194495, Hillwig *et al*. [15] for BD+60497 and HD 17505Aa, Tomkin [16] for HDE 284414 and Howarth *et al*. [17] for LZ Cep(HD 209481), respectively. Here the errors of the combined spectroscopic elements in Tables 2, 4, 6, 8 and 10 are obtained by the help of orbital parameters errors. See again Eqs. (3), (15) and (16) in Karami and Teimoorinia [4].

CONCLUSIONS

A Probabilistic Neural Network to derive the orbital elements of spectroscopic binary stars was applied. PNNs are used in both regression (including parameter estimation) and classification problems. However, one can discretize a continuous regression problem to such a degree that it can be represented as a classification problem [20,21], as we did in this work.

Using the measured V_R data of HD 194495, BD+60497, HD 17505Aa, HDE 284414 and LZ Cep(HD 209481) obtained by Çakırlı *et al*. [14], Hillwig *et al*. [15], Tomkin [16] and Howarth *et al*. [17], we find the orbital elements of these systems by the PNN. Our numerical results show that the results obtained for the orbital and spectroscopic parameters agree well with those obtained by others using traditional methods.

This method is applicable to orbits of all eccentricities and inclination angles. In this method the time consumed is considerably less than the method of Lehmann-Filhés. It is also more accurate as the orbital elements are deduced from all points of the velocity curve instead of four in the method of Lehmann-Filhés. The present method enables one to vary all of the unknown parameters γ,K,e and ω simultaneously instead of one or two of them at a time. It is possible to make adjustments in the elements before the final result is obtained. There are some cases, for which the geometrical methods are inapplicable and in these cases the present one may be found useful. One such case would occur when observations are incomplete because certain phases could have not been observed. Another case in which this method is useful is that of a star attended by two dark companions with commensurable periods. In this case the resultant velocity curve may have several unequal maxima and the geometrical methods fail altogether.

ACKNOWLEDGEMENTS

This work has been supported financially by Islamic Azad University, Marivan Branch, Iran.

REFERENCES

1. Lehmann-Filhés, R., 1894. Ueber Die Bestimmung Einer Doppelsternbahn Aus Spectroskopischen Messungen Der Im Visionsradius Liegenden Geschwindigkeitscomponente. AN., 136: 17-30.
2. Sterne, T.E., 1941. Notes on Binary Stars. V. The Determination by Least-Squares of the Elements of Spectroscopic Binaries. PNAS., 27: 175-181.
3. Petrie, R.M., 1960. Astronomical Techniques. Ed., Hiltner, W.A., University of Chicago Press, Chicago.
4. Karami, K. and H. Teimoorinia, 2007. Velocity Curve Analysis of the Spectroscopic Binary Stars by the Non-linear Least Squares. Ap. and SS., 311: 435-442.
5. Karami, K. and R. Mohebi, 2007a. Velocity Curve Analysis of Spectroscopic Binary Stars AI Phe, GM Dra, HD 93917 and V502 Oph by Nonlinear Regression. ChJAA., 7: 558-564.
6. Karami, K. and R. Mohebi, 2007b. Velocity Curve Analysis of Spectroscopic Binary Stars PV Pup, HD141929, EE Cet and V921 Her by Nonlinear Regression. JApA., 28: 217-230.
7. Karami, K. and R. Mohebi, 2009. Velocity Curve Studies of Spectroscopic Binary Stars V380 Cygni, V401 Cyg, V523 Cas, V373 Cas and V2388 Oph. JApA., 30: 153-163.
8. Karami, K., R. Mohebi and M.M. Soltanzadeh, 2008. Application of a New Non-linear Least Squares Velocity Curve Analysis Technique for Spectroscopic Binary Stars. Ap and SS., 318: 69-71.
9. Mohseni-Astani, R., P. Haghparast and S. Bidgoli-Kashani, 2010. Assessing and Predicting the Soil Layers Thickness and Type Using Artificial Neural Networks-Case Study in Sari City of Iran. Middle-East J. Sci. Res., 6(1): 62-68.
10. Sajid, M.R., F. Maqsood and M. Rani, 2011. Determinants of Fertility: A Neural Network Approach. Middle-East J. Sci. Res., 8(2): 440-449.
11. Hakimpoor, H., K.A. Bin Arshad, H. Hon Tat, N. Khani and M. Rahmandoust, 2011. Artificial Neural Networks' Applications in Management. World Appl. Sci. J., 14(7): 1008-1019.
12. Jalalkamali, A. and N. Jalalkamali, 2011. Application of Hybrid Neural Modeling and Radial Basis Function Neural Network to Estimate Leakage Rate in Water Distribution Network. World Appl. Sci. J., 15(3): 407-414.
13. Hussain Naveed, M., S.S Ahmad, S. Khalid and S. Khan, 2010. Development of Prediction Model for the Concentration Level of Air Toxin in the City of Rawalpindi Using Artificial Neural Network. World Appl. Sci. J., 10(1): 01-08.
14. Çakırlı, Ö., E. Spahi and C. Íbanoglu, 2011. Absolute Properties of the Neglected Eclipsing B-type Binary HD194495. New Astron., doi:10.1016/j.newast. 2011. 06.012J.
15. Hillwig, T.C., D.R. Gies, W.G. Bagnuolo, J.W. Huang, M.V. Mcswain and D.W. Wingert, 2006. Binary and Multiple O-type Stars in the Cassiopeia OB6 Assocation. Aj., 639: 1069-1080.

16. Tomkin, J., 2005. The Duble-lined System HDE 284414. Obs., 125: 232-238.
17. Howarth, I.D. and D.J. Stickland, 1991. Spectroscopic Binary Orbits from Ultraviolet Radial Velocities. Obs., 111: 167-178.
18. Smart, W.M., 1990. Textbook on Spherical Astronomy. Sixth Ed., Revised by Green, R.M., Cambridge Univ.
19. Bazarghan, M., H. Safari, D.E. Innes, E. Karami and S.K. Solanki, 2008. A Nanoflare Model for Active Region Radiance: Application of Artificial Neural Networks. A and A., 492: L13-L16.
20. Specht, D.F., 1988. In Proc IEEE International Conference on Neural Networks.
21. Specht, D.F., 1990. Probabilistic Neural Networks. Neural Networks, 3: 109-118.
22. Parzen, E., 1962. On Estimation of a Probability Density Function and Mode. Annals of Mathematical Statistics, 33: 1065-1076.